

**Material:** Ferritic Steel: F82H  
**Property:** Damage (dpa) versus He concentration (appm)  
**Condition:** Helium doped  
**Data:** Experimental

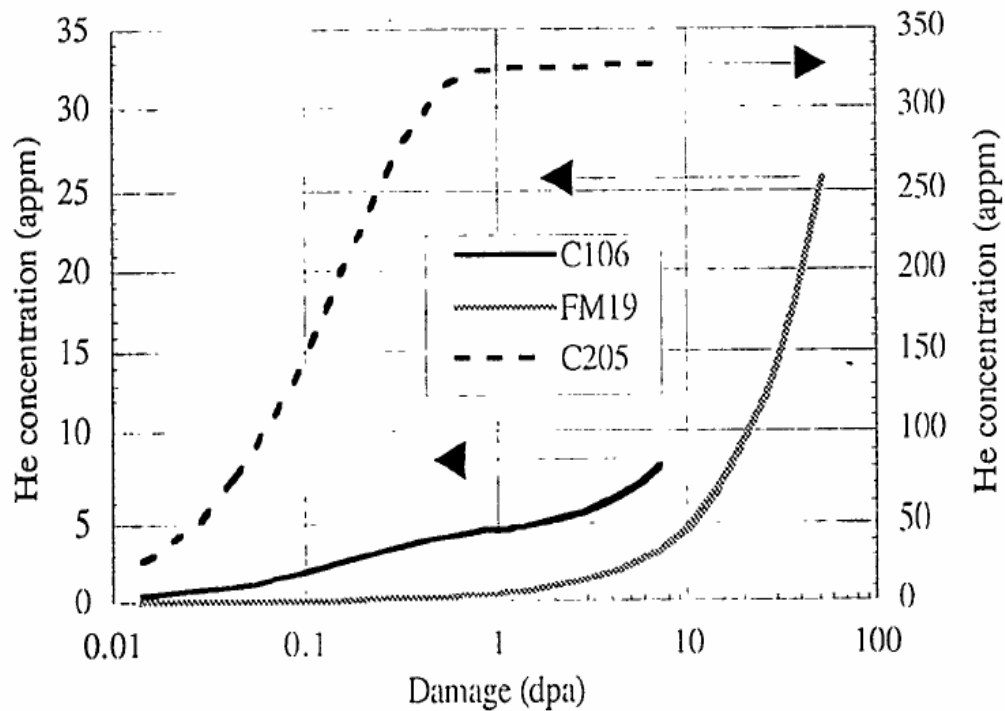


Figure 1 Dose dependence of He concentration in F82H-std (C106, FM19) and F82H+<sup>10</sup>B (C205). He concentrations are 8, 26 and 330 appm in C106, FM19, and C205, respectively.

**Source:**

Fusion Materials Semiannual Progress Report, 25, 1998, 175-182

**Title of paper (or report) this figure appeared in:**

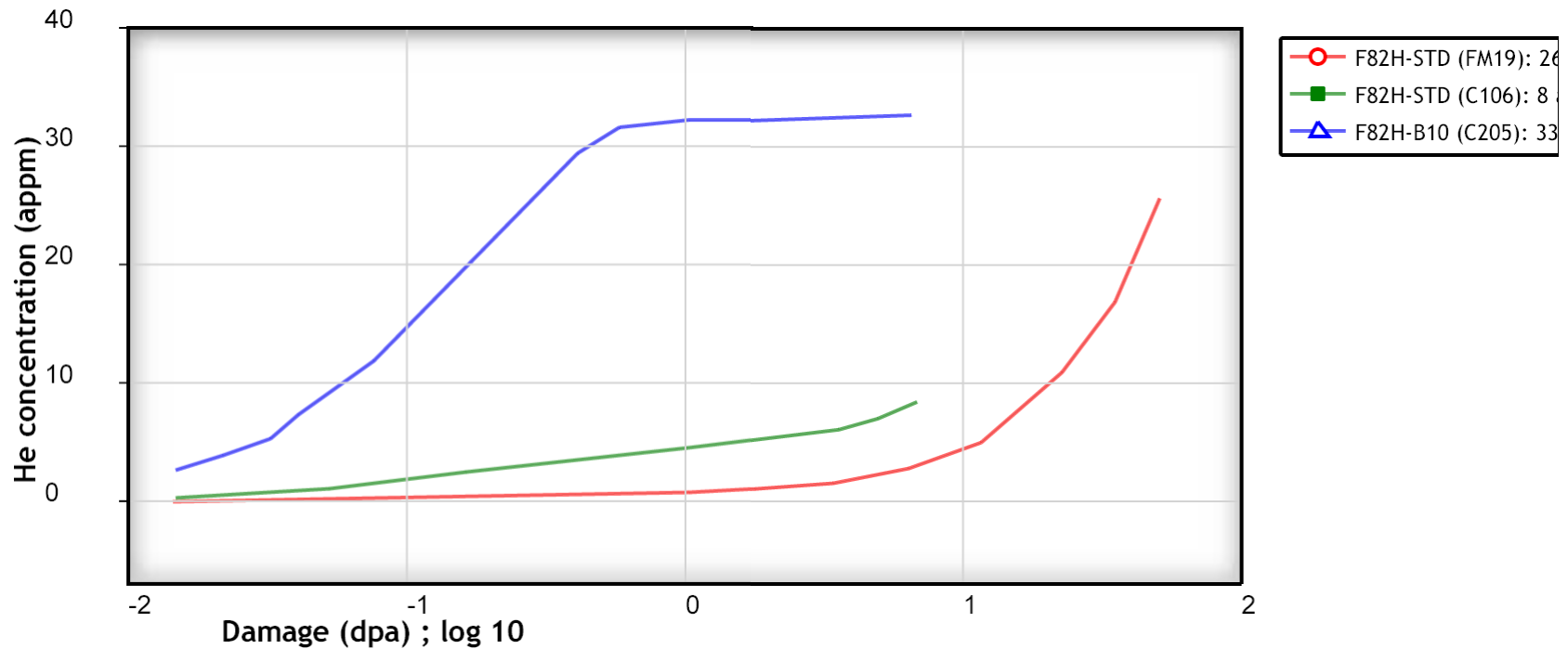
Swelling of F82H Irradiated at 673 K to 7dpa in HFIR

**Author of paper or graph:**

Y. Miwa, E. Wakai, K. Shiba, N. Hashimoto, J. P. Robertson, and A. F. Rowcliffe

**Caption:**

Dose dependence of He concentration in F82H-STD (C106, FM19) and F82H-B10 (C205). He concentrations are 8, 26 and 330 appm in C106, FM19, and C205 respectively.



**Dose dependence of He concentration in F82H-STD (C106, FM19) and F82H-B10 (C205). He concentrations are 8, 26 and 330 appm in C106, FM19, and C205 respectively**

**Reference:**

**Author:** *Y. Miwa, E. Wakai, K. Shiba, N. Hashimoto, J. P. Robertson, and A. F. Rowcliffe*

**Title:** *Swelling of F82H Irradiated at 673 K to 7dpa in HFIR*

**Source:** *Fusion Materials Semiannual Progress Report, 1998, Volume 25, Page 175-182,*  
[\[PDF\]](#)

**Swelling of F82H irradiated at 673 K to 7 dpa in HFIR** - Y. Miwa, E. Wakai, K. Shiba (Japan Atomic Energy Research Institute), N. Hashimoto, J. P. Robertson and A. F. Rowcliffe (Oak Ridge National Laboratory)

## OBJECTIVE

The objective of this work is to study the effect of neutron irradiation on swelling behavior of reduced activation ferritic/martensitic steels for first wall applications in fusion energy system.

## SUMMARY

A reduced activation ferritic/martensitic steel F82H (F82H-std) and a heat with the addition of isotope  $^{10}\text{B}$  (F82H+ $^{10}\text{B}$ ) were irradiated at 673 K to 7 and 51 dpa in HFIR. The swelling behavior of these alloys was examined by transmission electron microscopy. In the F82H-std irradiated to 7 dpa, small cavities ( $\sim 8$  nm in diameter) were observed in lath cells, but not on the interfaces of lath boundaries or precipitates. The cavity number density ( $N_c$ ) was about  $4 \times 10^{21} \text{ m}^{-3}$ . The swelling was about 0.2%. In the F82H+ $^{10}\text{B}$  irradiated to 7 dpa, smaller cavities ( $\sim 6$  nm in diameter.) were observed in lath cells, and some cavities occurred on the interfaces of lath boundaries or small precipitates. The  $N_c$  was about  $1.5 \times 10^{22} \text{ m}^{-3}$ , and the swelling was about 0.2%. In the F82H-std irradiated to 51 dpa, large and small cavities were observed in lath cells, but not on the interfaces of lath boundaries or precipitates. The  $N_c$  was about  $1 \times 10^{21} \text{ m}^{-3}$ , and the swelling was about 0.6%.

## PROGRESS AND STATUS

### Introduction

The reduced activation ferritic/martensitic steel F82H is one of the candidate materials for the first wall structure of fusion reactors. The effect of neutron irradiation on mechanical properties and microstructures in F82H is being examined in the Japan/US collaborative program on fusion reactor materials. The swelling behavior of F82H irradiated at 673 K up to 51 dpa is presented in this report.

## Experimental Procedure

Two types of F82H, one containing a low concentration of normal boron (F82H-std) and the other containing an addition of isotopic  $^{10}\text{B}$  (F82H+ $^{10}\text{B}$ ), were prepared to examine the effect of helium on the microstructures. The chemical compositions and notations of these alloys are given in Table 1. C106 and FM19 are F82H-std specimens, and C205 is the F82H+ $^{10}\text{B}$  specimen. Heat treatment conditions of each specimen are listed in Table 2.

Standard transmission electron microscopy specimens of 3 mm in diameter were punched out from 0.25-mm-thickness plates. These specimens were irradiated at about 673 K in HFIR target position in the capsule of HFIR-MFE-JP12/position 8 [1] and HFIR-MFE-JP20/position 9 [2]. The resulting thermal and fast neutron fluences, taking into account the specimen position in reactor are  $1.08 \times 10^{27} \text{ n/m}^2$  ( $E < 0.5 \text{ eV}$ ) and  $3.65 \times 10^{26} \text{ n/m}^2$  ( $E > 1 \text{ MeV}$ ) for HFIR-MFE-JP12 [3] and  $1.83 \times 10^{26} \text{ n/m}^2$  ( $E < 0.5 \text{ eV}$ ) and  $5.16 \times 10^{25} \text{ n/m}^2$  ( $E > 1 \text{ MeV}$ ) for HFIR-MFE-JP20 [4], respectively. These fluences correspond to 51.3 and 7.4 dpa for HFIR-MFE-JP12 and HFIR-MFE-JP20, respectively. The dose dependence of He generation in each specimen is shown in Figure 1.

Microstructural observation was carried out using a JEM-2000FX transmission electron microscope with a  $\text{LaB}_6$  gun operated at 200 kV. The root mean cube of cavity radius,  $r_{\text{RMC}}$ , was obtained by

$$r_{\text{RMC}} = \{(\sum r_i^3)/N\}^{1/3}$$

The distribution of cavities was not uniform, so that the cavity number density ( $N_c$ ) and the swelling were measured in cavity rich region in order to estimate the maximum swelling.

## Results and Discussion

### Swelling in F82H-std (C106) irradiated to 7 dpa

Figures 2(a)~(c) show the cavity distribution in F82H-std irradiated to 7 dpa. The calculated He concentration is about 8 appm. As seen in Figures 2(a) and (b), small cavities were observed in lath cells, and aligned along dislocation lines. Small cavities were also observed on dislocation loops that were formed during irradiation. A few cavities were observed on the interfaces of small precipitates, but no cavities were observed on larger

precipitates. Cavities were not observed on the lath boundaries (Figure 2(c)). The width of cavity free zone from lath boundaries was about 50 nm. Relatively larger cavities were faceted which suggested some conversion to bias-driven voids was occurring.

Figure 3 shows the size distribution of cavities. The diametral size distribution had a peak at 5 nm with a maximum diameter of about 20 nm. The  $r_{\text{RMC}}$  and  $N_c$  were about 4.3 nm and about  $4.0 \times 10^{21} \text{ m}^{-3}$ , respectively. The swelling was about 0.2%.

#### Swelling in F82H+ $^{10}\text{B}$ (C205) irradiated to 7 dpa

Figures 4(a)~(c) show the cavity distribution in F82H+ $^{10}\text{B}$  irradiated to 7 dpa. The calculated He concentration is about 330 appm. Cavities were observed associated with dislocations within the lath cells. The average diameter was smaller and the number density higher than in the F82H-std (Figures 4(a) and (b)). Some cavities were observed on the interfaces on lath boundaries or small precipitates (Figures 4(b) and (c)). All cavities were spherical with no evidence of facetting.

Figure 5 shows the size distribution of cavities. The diametral size distribution had a peak at about 4 nm with a maximum diameter of about 15 nm. These are smaller than those in C106. The fraction of larger cavities ( $\sim 10$  nm in diameter) was smaller than that in C106. The  $r_{\text{RMC}}$  and  $N_c$  were about 3.1 nm and about  $1.5 \times 10^{22} \text{ m}^{-3}$ , respectively. The swelling was about 0.2%. The  $N_c$  was higher and  $r_{\text{RMC}}$  was smaller than that in C106, swelling was about the same as that in C106. The addition of  $^{10}\text{B}$  results in He generation of about 320 appm from  $^{10}\text{B}(n, \alpha)^7\text{Li}$  reaction in steel at an early stage (about 1 dpa) of the neutron irradiation up to 7 dpa. The rapid generation of helium in  $^{10}\text{B}$ -doped material (Figure 1) is thought to be directly responsible for the four times increase in the measured cavity density.

#### Swelling in F82H-std (FM19) irradiated to 51 dpa

Figures 6(a)~(c) show the cavity distribution in F82H-std irradiated to 51 dpa. The calculated He concentration is about 26 appm. As seen in Figures 6(a)~(c), cavities were observed in lath cells, and not on lath boundaries or precipitates/matrix interfaces. The width of the void free zone at lath boundaries was about 50 nm, which is similar to that in F82H-std irradiated to 7 dpa (C106). Small and large cavities are shown in Figure 6(b); the

larger cavities were frequently observed at dislocation kinks or bowed-out dislocations. Many of the small cavities occurred in close proximity to a large cavity, frequently less than a small cavity diameter away.

Figure 7 shows the size distribution of cavities. The diametral size distribution has a peak at about 8 nm, and the maximum diameter is about 55 nm. These are much larger than those in C106. The  $r_{\text{RMC}}$  and  $N_c$  were about 11 nm and about  $1 \times 10^{21} \text{ m}^{-3}$ , respectively. The  $N_c$  is lower and  $r_{\text{RMC}}$  is larger than that in C106. The swelling was about 0.6 %, significantly larger than that in the 7 dpa specimen.

The details of microstructures of a series of F82H alloys irradiated at 673 K to 54 dpa are reported by Wakai et. al. elsewhere [5] in this report.

## ACKNOWLEDGMENTS

The authors would like to thank Dr. S. J. Zinkle in ORNL for fruitful discussion, and Messrs. L. T. Gibson, A. T. Fisher, J. J. Duff, and members of the 3025E hot cells for technical support.

## REFERENCES

- [1] R. L. Senn, Fusion Reactor Materials Semiannual Progress Report, DOE/ER-0313/5, p.6 (1988)
- [2] J. E. Pawel, Fusion Reactor Materials Semiannual Progress Report, DOE/ER-0313/15, p.3 (1993)
- [3] L. R. Greenwood, Fusion Reactor Materials Semiannual Progress Report, DOE/ER-0313/23, p.301 (1997)
- [4] L. R. Greenwood, Fusion Reactor Materials Semiannual Progress Report, DOE/ER-0313/23, p.305 (1997)
- [5] E. Wakai, in this semi-annual report.

Table 1 Chemical compositions (mass %)

	C	Si	Mn	P	S	Cr	W	V	Ta	T. Al	T. N	Ni	Ti	B
FM19	0.100	0.14	0.49	0.001	0.001	7.44	2.0	0.20	0.04	0.019	0.002			tr.*1
C106	0.097	0.09	0.07	0.002	0.003	7.46	2.1	0.18	0.03	0.014	0.004	0.03	0.008	0.0004
C205	0.098	0.17	0.5	0.001	0.001	7.23	2.1	0.22	0.04	0.021	0.002			0.0058*2

\*1: tr. means trace quantity.

\*2: all boron is  $^{10}\text{B}$ .

Table 2 Heat treatment conditions

	Normalizing	Tempering
FM19	1313 K / 0.5 h / AC	1013 K / 2 h / AC
C106	1313 K / 0.667 h / AC	1013 K / 1.5 h / AC
C205	1313 K / 0.5 h / AC	1013 K / 1.5 h / AC

AC: air-cooling. Normalizing and tempering was carried out in vacuum.

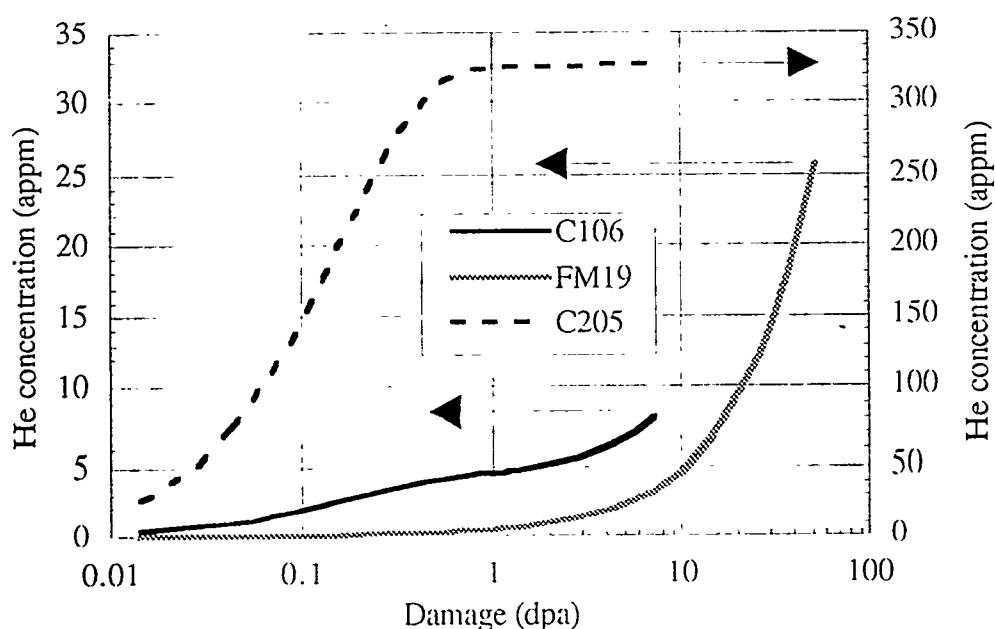


Figure 1 Dose dependence of He concentration in F82H-std (C106, FM19) and F82H+ $^{10}\text{B}$  (C205). He concentrations are 8, 26 and 330 appm in C106, FM19, and C205, respectively.

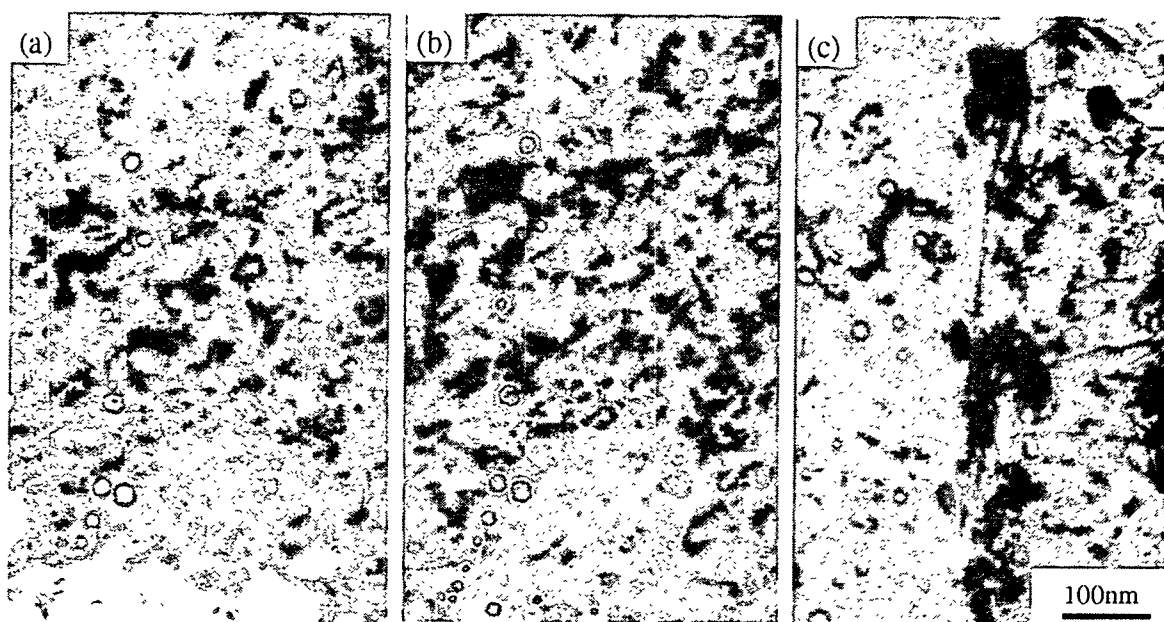


Figure 2 Cavities in F82H-std irradiated at 673 K to 7 dpa. The calculated He concentration is about 8 appm. (a) and (b): Underfocus and overfocus image in the same position of matrix. (c): Cavities near lath boundary.

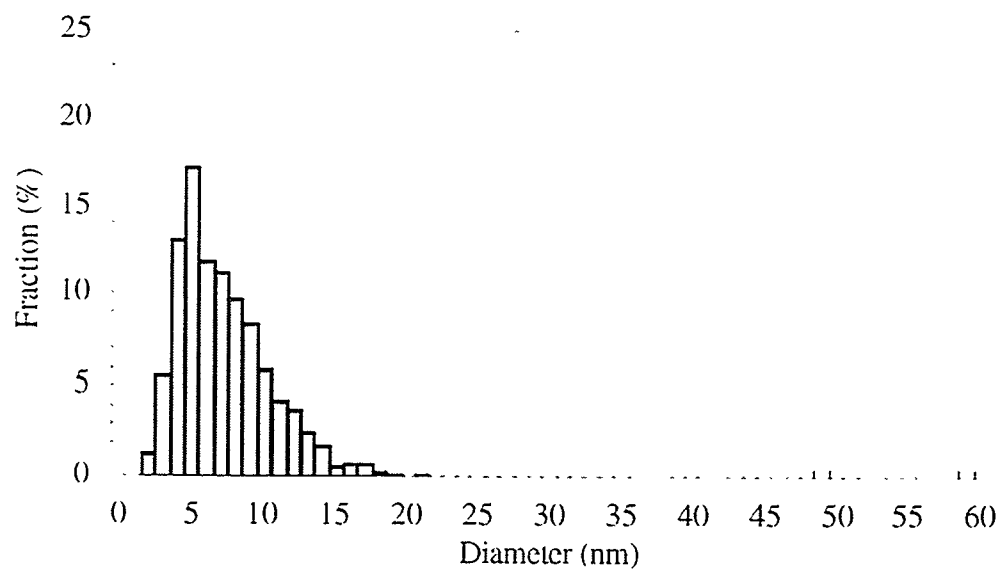


Figure 3 Cavity size distribution in F82H-std irradiated at 673 K to 7 dpa.



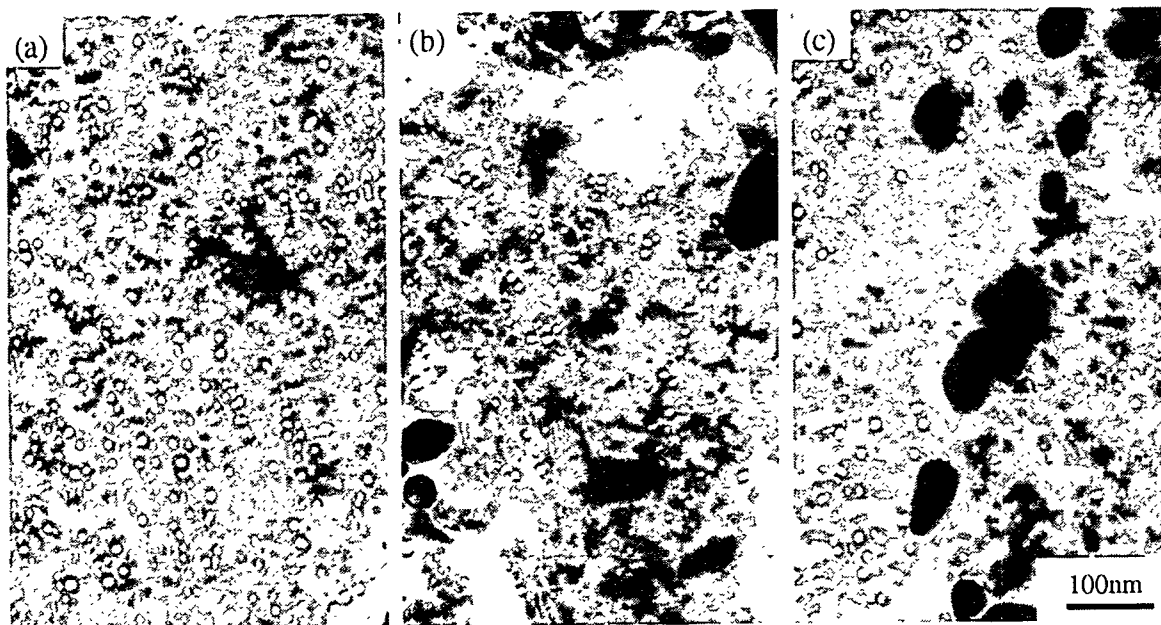


Figure 4 Cavities in F82H+ $^{10}\text{B}$  irradiated at 673 K to 7 dpa.

The calculated He concentration is about 330 appm. (a) and (b): Many cavities were observed along dislocations. (c): Some cavities on small precipitates and lath boundaries.

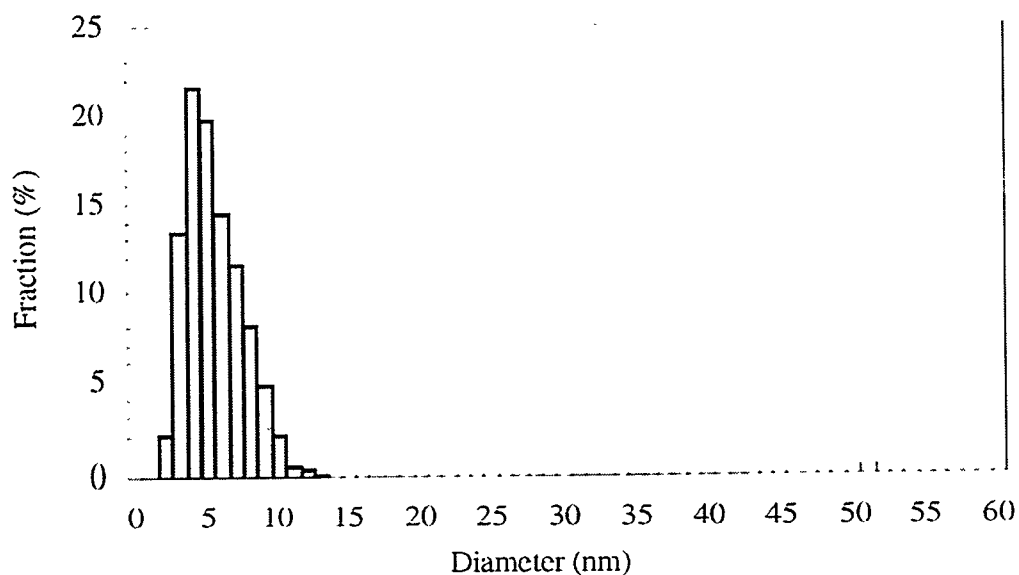


Figure 5 Cavity size distribution in F82H+ $^{10}\text{B}$  irradiated at 673 K to 7 dpa.

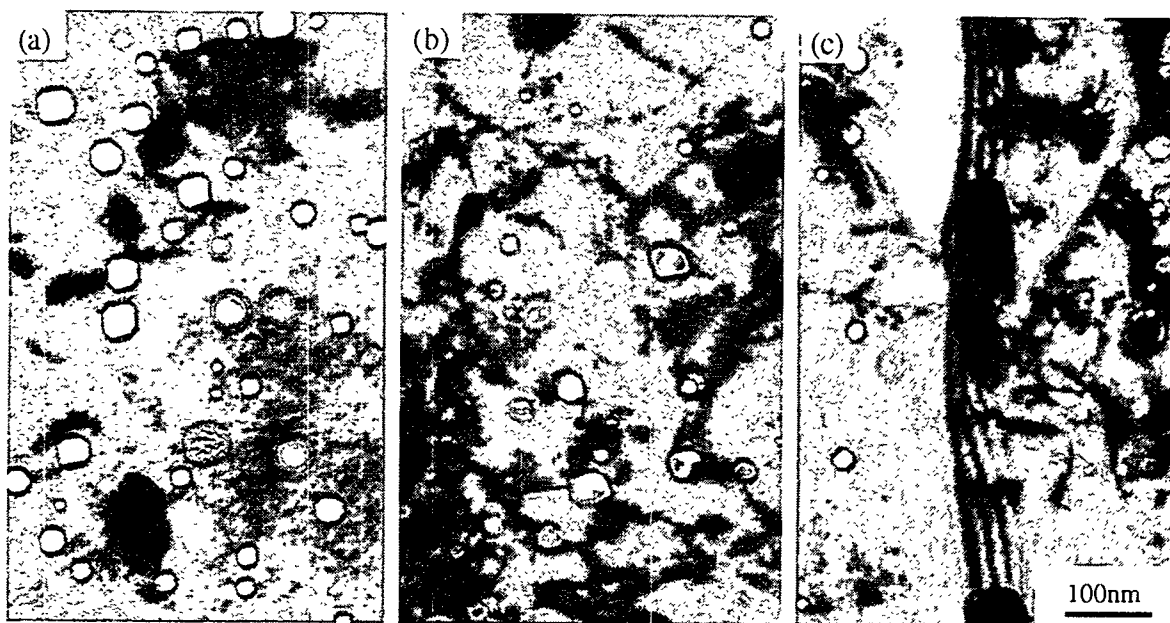


Figure 6 Cavities in F82H-std irradiated at 673 K to 51 dpa.

The calculated He concentration is about 26 appm. (a): Cavities in the matrix ( $s \gg 0$ ). (b): Cavities in matrix ( $s \sim 0$ ), and large cavities were observed at dislocation. (c): No cavities near lath boundaries.

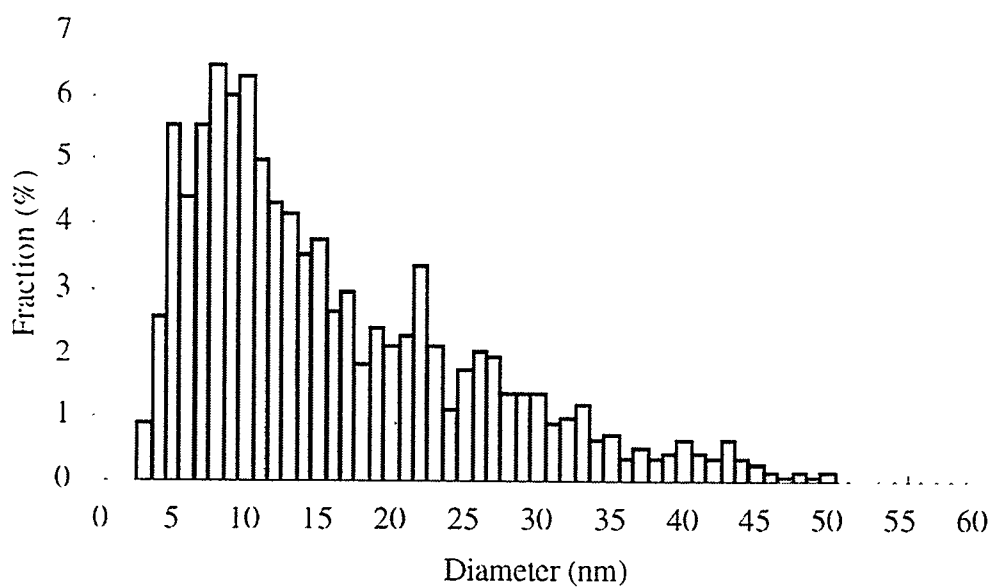


Figure 7 Cavity size distribution in F82H-std irradiated at 673 K to 51 dpa.